Draft version December 14, 2018
Typeset using LaTeX **twocolumn** style in AASTeX62

Solving the diffusion equation as a partial differential equation using different numerical solvers

Hans Erlend Bakken Glad, Stig-Nicolai Foyn, Torbjørn Lode Gjerberg, and Christer Dreierstad

ABSTRACT

In this paper we will apply the diffusion equation to a one and two dimensional system to study how temperature changes over time as we apply different boundary and initial conditions, and lastly sources of heat. For the one dimensional case we time evolve the diffusion equation using the Forward Euler scheme, and with two implicit schemes; Backward Euler and Crank-Nicolson. By transforming the equations in the latter two schemes we time evolve the system by solving a tridiagonal matrix system. We see that Backward Euler offers the best numerical accuracy when increasing the resolution of the calculations. When expanding the model into two dimensions we expand the Forward Euler scheme. To use Backward Euler we apply Jacobi's iterative method to our numerical solver. We find that Backward Euler has a far better numerical accuracy than Forward Euler. Finally we apply the methods to a two dimensional lithosphere. The lithosphere is modeled in three stages: 1) steady state 2) with inner heat production 3) combining inner with an outer heat production, where the outer heat comes from a slab beneath the lithosphere. Our results for this model are stable in the centre of the system.

Keywords: Geophysics, computational science: partial differential equations, diffusion equation — methods: Forward Euler, Backward Euler, Crank-Nicholson, Jacobi's iterative

1. INTRODUCTION

In this study we use the diffusion equation to model the temperature gradient in a material over time. The diffusion equation is a partial differential equation, and it is solved using three different numerical methods: the explicit Forward Euler (FE) scheme, the implicit Backward Euler (BE) scheme and the Crank-Nicolson (CN) scheme. These schemes are implemented using the programming language C++. The accuracy of these methods are then determined by comparing with the analytical solution.

The diffusion equation is initially implemented in one dimension, with different boundary conditions at the two ends. This can be interpreted as an infinitely thin rod where energy is being transported into the system at one end, and energy being transported out on the other end. This means that over time the energy spreads along the rod, which causes a temperature difference along the rod. Our model is also extended to two spatial dimensions. We first implement this with boundary conditions such that there is a energy being transported in from the bottom, and transported out from the other ends. When we compare the numerical implementation against the analytical in two dimensions, we simplify the model such that there is no energy being transported into the system, this allows for an easier derivation of an analytical solution.

The paper will first outline the theory behind the diffusion equation and how it is solved numerically, then we look at the properties of our numerical solvers. The precision of our methods are then evaluated with the help of analytical solutions for both the one dimensional, and two dimensional case. In the one-dimensional case, we find that the explicit FE method is significantly less accurate compared to the implicit methods. Expanding the two dimensional model to a lithosphere we scale the heat equation by introducing dimensionless variables.

2. METHOD

2.1. *Diffusion Equation*

The model we employ to describe heat diffusion is the diffusion equation:

$$\vec{\nabla} k \vec{\nabla} T(\mathbf{x}, t) = c_P \rho \frac{\partial T(\mathbf{x}, t)}{\partial t} \tag{1}$$

where c_P is the specific heat, ρ is the density of the material and k is the thermal conductivity. We arrive at this equation when we assume heat diffusion is proportional to a temperature gradient.

In order to discretize and solve this system we scale the equations. The first case is the 1-dimensional case. First we gather all the constants in the diffusion equation and substitute them as D;

$$\frac{\partial^2 T(x,t)}{\partial x^2} = D \frac{\partial T(x,t)}{\partial t}$$

and introduce a dimensionless variable $\lambda = x/\hat{x}$, where $\hat{x}$ has unit length. Inserting the previous expression solved for x; $x = \lambda\hat{x}$, into the diffusion equation, we see that

$$\frac{\partial^2 T(\hat{x},t)}{\partial \hat{x}^2} = \lambda^2 D \frac{\partial T(\hat{x},t)}{\partial t}.$$

λ in the previous equation is just a constant, and we choose this to be such that $\lambda^2 D = 1$, with the purpose of scaling the equation (we also set $\hat{x} = x$)

$$\frac{\partial^2 u(x,t)}{\partial x^2} = \frac{\partial u(x,t)}{\partial t}, t > 0, x \in [0, L]. \tag{2}$$

For the 2-dimensional equation we make a similar argument, and we get a factor $1/\lambda^2$ for both the second partial derivative for x and y when scaling, multiplying by λ^2 as above we get the equation

$$\frac{\partial^2 T(\hat{x},\hat{y},t)}{\partial \hat{x}^2} + \frac{\partial^2 T(\hat{x},\hat{y},t)}{\partial \hat{y}^2} = \lambda^2 D \frac{\partial T(\hat{x},t)}{\partial t}.$$

We scale the above equation as previous and end up with the scaled equation for the two dimensional diffusion equation:

$$\frac{\partial^2 u(x,y,t)}{\partial x^2} + \frac{\partial^2 u(x,y,t)}{\partial y^2} = \frac{\partial u(x,y,t)}{\partial t}. \tag{3}$$

2.2. *Explicit Scheme*

The FE method uses the standard approximations of the derivative. In the 1 spacial dimension case (1+1 dimensions) we have the approximation for the time derivative

$$\frac{\partial u}{\partial t} \approx \frac{u(x, t+\Delta t) - u(x,t)}{\Delta t} = u_t,$$

and the spatial derivative

$$\frac{\partial^2 u}{\partial x^2} \approx \frac{u(x+\Delta x, t) - 2u(x,t) + u(x-\Delta x, t)}{\Delta x^2} = u_{xx}.$$

We discretize u_{xx} and u_t, which gives the following expressions

$$u_t = \frac{u(x_i, t_l + \Delta t) - u(x_i, t_l)}{\Delta t}$$

and

$$u_{xx} = \frac{u(x_i + \Delta x, t_l) - 2u(x_i, t_l) + u(x_i - \Delta x, t_l)}{\Delta x^2}.$$

Introducing the notation $u(x_i, t_l) = u_i^l$ ($u_{i,j}^l$ for two spatial dimensions x, y), and setting the previous two equation equal by Eq. (2), we solve the equation for the solution in the next time step u_i^{l+1}, which yields

$$\frac{u_i^{l+1} - u_i^l}{\Delta t} = \frac{u_{i+1}^l - 2u_i^l + u_{i-1}^l}{\Delta x^2}.$$

Setting $\alpha = \frac{\Delta t}{\Delta x^2}$ and solving for u_i^{l+l} our u_i for the next time step is

$$u_i^{l+l} = (1 - 2\alpha)u_i^l + \alpha(u_{i+1}^l + u_{i-1}^l) \tag{4}$$

in Eq. (4) all the terms on the right hand side are known when we insert initial conditions. However the explicit Euler method has a stability requirement in one dimension that must be met

$$\frac{\Delta t}{\Delta x^2} \leq \frac{1}{2}. \tag{5}$$

Expanding the scheme to two dimensions the equation $u \to u(x,y,t)$, which is $u(x_i, y_j, t_j) = u_{i,j}^l$ when discretized. The second term on the right in the 2D diffusion equation, Eq. (3), is approximated as with the second derivative with respect to x;

$$\frac{\partial^2 u}{\partial y^2} \approx \frac{u_{i,j+1}^l - 2u_{i,j}^l + u_{i,j-1}^l}{\Delta y^2},$$

and inserting $u_{i,j}^l$ into Eq. (3) we get

$$\frac{u_{i,j}^{l+1} - u_{i,j}^l}{\Delta t} = \frac{u_{i+1,j}^l - 2u_{i,j}^l - u_{i-1,j}^l}{\Delta x^2} + \frac{u_{i,j+1}^l - 2u_{i,j}^l - u_{i,j-1}^l}{\Delta y^2}.$$

We choose $\Delta x = \Delta y$, and set $\alpha = \Delta t/\Delta x^2$ as before. Solving the equation for the solution of the next time step gives

$$u_{i,j}^{l+l} = (1 - 4\alpha)u_{i,j}^l + \alpha(u_{i+1,j}^l + u_{i-1,j}^l + u_{i,j+1}^l + u_{i,j-1}^l)$$

where every term on the right hand side is known when we have appropriate initial conditions for both x and y. Solving this as a tridiagonal matrix system is shown in (Project 1 2018).

When moving to two dimensions the stability requirement changes as well to

$$\frac{\Delta t}{\Delta x^2} \leq \frac{1}{4} \tag{6}$$

One final aspect of the Explicit scheme is the truncation error. We get a truncation error because we truncate the expansion

$$f(t + \Delta t) = f(t) + \Delta t f^{'}(t) + \mathcal{O}(\Delta t^2)$$

at the first order term. Solving for $f^{'}(x)$

$$f^{'}(t) = \frac{f(t) - f(t + \Delta t)}{\Delta t} + \mathcal{O}(\Delta t)$$

where we find that the error is of order Δt. Finding the error of the second order derivative requires an expansion

$$f(x \pm \Delta x) = f(x) \pm \Delta x f^{'}(x) \pm \frac{\Delta x^2}{2} f^{''}(x) \pm \frac{\Delta x^3}{6} f^{'''}(x) + \mathcal{O}(\Delta x^4)$$

which we rewrite for convenience to

$$f_{\pm h} = f \pm h f^{'} + \frac{h^2}{2} f^{''} \pm \frac{h^3}{6} f^{'''} + \mathcal{O}(h^4)$$

where $h \equiv \Delta x$. Subtracting $f_{\pm}$ and solving for $f^{'}$ gives

$$f^{'} = \frac{f_h - f_{-h}}{2h} + \frac{h^2}{6} f^{'''} + \mathcal{O}(h^3)$$

Inserting this in Taylor expansion of the third order and leaves the expression

$$f_h - 2f + f_{-h} = h^2 f'' + \mathcal{O}(h^4)$$

Solving for $f^{''}$ we get the the second order derivative

$$f^{''} = \frac{f_h - 2f + f_{-h}}{h^2} + \mathcal{O}(h^2) \tag{7}$$

on the same form as the spatial part of our explicit method. This means that the truncation error in the spatial part of the explicit method is Δx^2.

2.3. *Implicit Schemes*

2.3.1. *Backward Euler*

The discretized time derivative of the BE scheme is given by

$$\frac{\partial u}{\partial t} \approx \frac{u(x,t) - u(x,t-\Delta t)}{\Delta t} = \frac{u_i^l - u_i^{l-1}}{\Delta t} = u_t, \tag{8}$$

and the for the spatial double derivative

$$\frac{\partial^2 u}{\partial x^2} \approx \frac{u(x+\Delta x,t) - 2u(x,t) + u(x-\Delta x,t)}{\Delta x^2},$$

which discretized becomes

$$\frac{\partial^2 u}{\partial x^2} \approx \frac{u_{i+1}^l - 2u_i^l + u_{i-1}^l)}{\Delta x^2} = u_{xx}, \tag{9}$$

where we have used the notation introduced in section 2.2. We again set the equations above equal by Eq. (2)

$$\frac{u_i^l - u_i^{l-1}}{\Delta t} = \frac{u_{i+1}^l - 2u_{il} + ui - 1^l}{\Delta x^2},$$

and then solving for the solution of the previous time step u_i^{l-1}:

$$u_i^{l-1} = -\alpha u_{i-1}^l + (1+2\alpha)u_i^l - \alpha u_{i+1}^l.$$

The previous equation can be written as a tridiagonal matrix system $Au_i^l = u_i^{l-1}$, where A is a tridiagonal matrix:

$$\begin{bmatrix} 1+2\alpha & -\alpha & 0 & \dots & 0 \\ -\alpha & 1+2\alpha & -\alpha & 0 & \dots \\ 0 & -\alpha & \dots & \dots & 0 \\ \dots & \dots & \dots & \dots & -\alpha \\ 0 & \dots & 0 & -\alpha & 1+2\alpha \end{bmatrix} \begin{bmatrix} u_1^l \\ u_2^l \\ \dots \\ u_{n-2}^l \\ u_{n-1}^l \end{bmatrix} = \begin{bmatrix} u_1^{l-1} \\ u_2^{l-1} \\ \dots \\ u_{n-2}^{l-1} \\ u_{n-1}^{l-1} \end{bmatrix}.$$

Expanding the scheme to two dimensions, we introduce the second partial derivative of u with respect to y, which is approximated as

$$\frac{\partial^2 u}{\partial y^2} \approx \frac{u(x,y+\Delta y,t) - 2u(x,y,t) + u(x,y-\Delta y,t)}{\Delta y^2},$$

which when discretized becomes

$$\frac{\partial^2 u}{\partial y^2} \approx \frac{u_{i,j+1}^l - 2u_{i,j}^l + u_{i,j-1}^l}{\Delta y^2} = u_{yy}. \tag{10}$$

Solving the scaled second order two dimensional diffusion Eq. (3) we get

$$\frac{u_{i,j}^l - u_{i,j}^{l-1}}{\Delta t} = \frac{u_{i+1,j}^l - 2u_{i,j}^l + u_{i-1,j}^l}{\Delta x^2} + \frac{u_{i,j+1}^l - 2u_{i,j}^l + u_{i,j-1}^l}{\Delta y^2},$$

where we again set $\Delta x^2 = \Delta y 2$ and $\alpha = \Delta t / \Delta x^2$. Solving the equation for the solution of the previous time step;

$$u_{i,j}^{l-1} = (1+4\alpha)u_{i,j}^l - \alpha(u_{i+1,j}^l + u_{i-1,j}^l + u_{i,j+1}^l + u_{i,j-1}^l),$$

which requires us to know the solution at the last time step. If we are to evolve u over time, we therefore have to implement an iterative method, which is discussed in section 2.4.

The truncation error in the implicit scheme comes from the same truncation for the explicit scheme, but with an expansion around $f(x-h)$ to find the backward derivative.

$$f(t-\Delta t) = f(t) + \Delta t f^{'}(t) + \mathcal{O}(\Delta t^2)$$

Solving for $f^{'}(t)$ gives the expression

$$f^{'}(t) = \frac{f(t) - f(t-\Delta t)}{\Delta t} + \mathcal{O}(\Delta t)$$

This expression has a truncation error of Δt as in the explicit case. For the spatial part the truncation error is also the same as for the explicit scheme. The spatial part of the implicit scheme is equal to the explicit scheme and is solved in Eq. (7).

2.3.2. *Crank-Nicolson*

For the CN scheme the approximation of the time derivative is given by

$$\frac{\partial u}{\partial t} \approx \frac{u(x,t+\Delta t)-u(x,t)}{\Delta t} = \frac{u_i^{l+1}-u_i^l}{\Delta t} = u_t,$$

when discretizing the equation. The approximation of the spatial double derivative is given by (where we have used $\alpha = \Delta t/\Delta x^2$)

$$\begin{aligned}\frac{\partial^2 u}{\partial x^2} \approx \frac{\alpha}{2} & u(x+\Delta x,t) - 2u(x,t) + u(x-\Delta x,t) \\ & + u(x+\Delta x,t+\Delta t) - 2u(x,t+\Delta t) \\ & + u(x-\Delta x,t+\Delta t),\end{aligned}$$

which when discretized becomes

$$\frac{\partial^2 u}{\partial x^2} \approx \frac{\alpha}{2} u_{i+1}^l - 2u_i^l + u_{i-1}^l + u_{i+1}^l - 2u_i^{l+1} + u_{i-1}^{l+1} = u_{xx}.$$

Setting these equations equal by Eq. (2), and solving for the solution of the next time step $l+1$ we get

$$(2+2\alpha)u_i^{l+1} - \alpha u_{i+1}^{j+1} - \alpha u_{i-1}^{j+1} = \alpha u_{i+1}^l + (2-2\alpha)u_i^l + \alpha u_{i-1}^l.$$

Transforming the CN scheme into a matrix equation, we can write the previous equation as

$$(2I - \alpha B)u_i^{l+1} = (2I + \alpha B)u_i^l,$$

where I is the identity matrix and the matrix B is a triangular matrix with constants along the upper, lower and central diagonal;

$$B = \begin{bmatrix} -2 & 1 & 0 & \dots & 0 \\ 1 & -2 & 1 & 0 & \dots \\ 0 & 1 & \dots & \dots & 0 \\ \dots & \dots & \dots & \dots & 1 \\ 0 & \dots & 0 & 1 & -2 \end{bmatrix}.$$

By multiplying by the inverse matrix $(2I+\alpha B)^{-1}$ from the left in the matrix equation above we get a tridiagonal matrix system

$$(2I+\alpha B)^{-1}(2I-\alpha B)u_i^{l+1} = u_i^l,$$

where $(2I+\alpha B)^{-1}(2I-\alpha B)$ is a matrix we can define as A, which brings to equation a known form: $Au_i^{l+1} = u_i^l$. To find the truncation errors in the CN method we need to expand $u(x-\Delta x, t+\Delta t)$, $u(x+\Delta x, t+\Delta t)$ and $u(x,t+\Delta t)$ around $\hat{t} = t + \Delta t/2$ in addition to the expansions done for Forward and Backward Euler. This can be seen in the lecture notes (Computational Physics 2015). The expansions are then added together like in the equations defining the CN scheme. As the last step we divide by Δt in the time derivative and Δx^2 in the spatial derivative, which leads to the truncation errors in terms of the approximations:

$$\begin{aligned}\left(\frac{\partial u(x,\hat{t})}{\partial t}\right)_{approx} &= \frac{\partial u(x,\hat{t})}{\partial t} + \mathcal{O}(\Delta t^2) \\ \left(\frac{\partial^2 u(x,\hat{t})}{\partial x^2}\right)_{approx} &= \frac{\partial^2 u(x,\hat{t})}{\partial x^2} + \mathcal{O}(\Delta x^2).\end{aligned}$$

All other relevant terms cancel out. Effective error then goes as $\mathcal{O}(\Delta t^2)$ and $\mathcal{O}(\Delta x^2)$.

2.4. *Jacobi's iterative method*

When implementing an implicit scheme in the two dimensional case, it is beneficial to use an iterative method like Jacobi's method. What the method essentially does is to approximate the diagonal values of a symmetric, positive definite or diagonally dominant matrix, to solve a linear matrix equation on the form $Ax = u$. However when we implement this method we are interested in developing the system over time. We start by using the same discretization as for the general 2D case, which is given by the equations for u_t, u_{xx} and u_{yy} seen in Eq. (8), (9) and (10). Note that the time-evolution u_t is given by the BE formula, but the calculations are not done backwards. To progress the equations are solved for $\alpha = \frac{\Delta t}{\Delta x^2}$:

$$u_{i,j}^l = \frac{\alpha(u_{i+1,j}^l + u_{i-1,j}^l + u_{i,j+1}^l + u_{i,j-1}^l) + u_{i,j}^{l-1}}{1+4\alpha}. \tag{11}$$

If we define $\Delta_{i,j}^l = (u_{i+1,j}^l + u_{i-1,j}^l + u_{i,j+1}^l + u_{i,j-1}^l)$ as the compact form, the equation can be shortened to:

$$u_{i,j}^l = \frac{1}{1+4\alpha}\left(\alpha\Delta_{i,j}^l + u_{i,j}^{l-1}\right).$$

This equation is iterated over, inserting the previous time solution as $u_{i,j}^{l-1}$ for every matrix that is sufficiently diagonal (the non diagonal terms are small enough to be approximated as zero). For $u_{i,j}^0$, we use an initial state chosen either by the boundary conditions or as done later on, chosen as steady the state.

To start Jacobi's iterative method an initial step is needed. In our algorithm this was determined to be the solution at a previous state in time. Our initial condition set up matrix of the initial state. After taking in the initial conditions we set up a matrix of temporary values. For each iteration, each term apart from the last on the right hand side in Eq. (11) we use the temporary values, which contain the initial guess of the solution, to find $u(i,j)$ at the current time step. The "guess" is now replaced with the $u(i,j)$ for the next iteration.

2.5. *Boundary conditions*

2.5.1. *One dimension*

In one dimension we consider the system to be a rod of length L where energy is being transported in from one end and transported out in the other. Choosing an initial relative temperature of the whole rod to be 0 (except on the ends discussed above), and setting the relative temperature of the energy end and the "cold" end to be 1 and 0 respectively, for all t. That is;

$$\begin{aligned} u(x,0) &= 0, \quad 0 < x < L \\ u(0,t) &= 0, \quad t \geq 0 \\ u(L,t) &= 1, \quad t \geq 0 \end{aligned}$$

2.5.2. *Two dimensions*

For the two dimensional case we consider a box where energy is being transported in from the bottom at $y = L, \forall x$, and the energy being transported out from the three other sides. The initial condition is 0 for x,y $\in (0, L)$.

$$\begin{aligned} u(x,y,0) &= 0, \quad 0 < x,y < L \\ u(0,y,t) &= 0, \quad 0 < y < L, \quad t \geq 0 \\ u(L,y,t) &= 0, \quad 0 < y < L, \quad t \geq 0 \\ u(x,0,t) &= 0, \quad 0 < x < L, \quad t \geq 0 \\ u(x,L,t) &= 1, \quad 0 < x < L, \quad t \geq 0 \end{aligned}$$

2.5.3. *Two dimensions, analytic case*

For the analytical solution of the two dimensional diffusion equation we choose the boundary condition to be 0 for all x, y. The analytical expression is discussed in section 2.6.2

$$\begin{aligned} u(x,y,0) &= \sin(\pi x/L)\sin(\pi y/L) \quad 0 < x,y < L \\ u(x,0,t) &= 0 \quad 0 < x < L, \quad t \geq 0 \\ u(x,L,t) &= 0 \quad 0 < x < L, \quad t \geq 0 \\ u(0,y,t) &= 0 \quad 0 < y < L, \quad t \geq 0 \\ u(L,y,t) &= 0 \quad 0 < y < L, \quad t \geq 0 \end{aligned}$$

2.5.4. *Temperature distribution in the lithosphere*

The initial condition for the lithosphere model we set the temperature only dependent upon depth. We set a relative temperature gradient from the top to bottom ranging from $8/1300 \to 1$. We consider the energy to be transported in from the bottom and out from the edges and top, as for the general two dimensional case discussed in section 2.5.2. The boundary conditions are:

$$\begin{aligned} T(x,y,0) &= y \quad 0 < x < L, \quad 8/1300 < y < 1 \\ T(0,y,t) &= 0, \quad 0 < y < L, \quad t \geq 0 \\ T(L,y,t) &= 0, \quad 0 < y < L, \quad t \geq 0 \\ T(x,0,t) &= 0, \quad 0 < x < L, \quad t \geq 0 \\ T(x,L,t) &= 1, \quad 0 < x < L, \quad t \geq 0 \end{aligned}$$

2.6. *Analytical solutions*

2.6.1. *One dimension*

The boundary conditions for our rod of length $L = 1$ are as discussed in section 2.5.1. We assume $u(x,t)$ to have a solution that that is a sum of two functions; $u(x,t) = v(x,t) + x \Rightarrow v(x,t) = u(x,t) - x$, where v has the following boundary conditions

$$\begin{aligned} v(x,0) &= 0, \quad 0 < x < L \\ v(0,t) &= 0, \quad t \geq 0 \\ v(L,t) &= 0, \quad t \geq 0, \end{aligned}$$

which satisfies the boundary conditions for $u(x,t)$. We further assume $u(x,t) = F(x)G(t)$ by separations of variables, inserting this into the scaled diffusion equation, Eq. (2), we get

$$\frac{1}{F}\frac{\partial^2 F}{\partial x^2} = \frac{1}{G}\frac{\partial G}{\partial t},$$

which is valid for all x and t, so both sides must equal a constant we name $-\lambda^2$. This gives the two solutions

$$F'' + \lambda^2 F = 0, \qquad G' + \lambda^2 G = 0,$$

with the general solutions

$$F(x) = A\sin(\lambda x) + B\cos(\lambda x), \qquad G(t) = Ce^{-\lambda^2 t}.$$

Looking at the boundary conditions for v, we see that $v(0,t) = F(0)G(t) = 0$;

$$G(t)A\sin(0) + G(t)B\cos(0) = G(t)B,$$

which means $B = 0$ to preserve the boundary conditions. Further we look at $v(L,t) = 0$, which means $0 = A\sin(\lambda L)G(t)$, which means $\lambda = n\pi/L$, because $\sin(n\pi) = 0 \; \forall \; n = 1, 2, 3, ...$ We have several solutions for each n, and gathering and renaming the constants in F and G to A_n we get the solution

$$u(x,t) = \sum_{n=1}^{\infty} A_n \sin(n\pi x/L)e^{-n^2\pi^2 t/L^2},$$

because the diffusion equation is linear, a superposition of solutions is also a solution of $u(x,t)$[1]. We find the A_n

[1] See (Computational Physics 2015) page 314.

by inverse Fourier transformation at $t = 0$;

$$A_n = \frac{2}{L}\int_0^L g(x)\sin(n\pi x/L)dx,$$

where $g(x) = v(x,0) = -x$, with $L = 1$ we get

$$A_n = -2\int_0^1 x\sin(n\pi x/L)dx = \frac{2\cos(\pi n)}{\pi n}.$$

The full analytical expression, with $L = 1$, for the 1D case is then

$$u(x,t) = \sum_{n=1}^{\infty}\frac{2\cos(\pi n)}{\pi n}\sin(n\pi x)e^{-n^2\pi^2 t}.$$

2.6.2. *Two dimensions*

To test the accuracy of our algorithms for the two dimensional solvers we solved Eq. (3) with the set of boundary conditions

$$u(0,y,t) = u(L,y,t) = 0, \quad t \geq 0$$
$$u(x,0,t) = u(x,L,t) = 0, \quad t \geq 0$$

as seen in section 2.5.2 and initial conditions

$$u(x,y,0) = \sin(\frac{\pi}{L}x)\sin(\frac{\pi}{L}y), \quad \text{for } x,y \in (0,L)$$

This choice of initial conditions simplifies the analytic solutions considerably allowing us to test the numerical solutions. These boundary and initial conditions correspond to a material with no sources of heat at any of the edges and an initial heat with a predisposition close to the center, i.e. the initial temperature decreases away from the center. As time increases the heat should begin to dissipate as all the boundaries act like drains. The steady state should be a system with zero temperature at all points.

The solution to the two dimensional, scaled diffusion equation with our boundary and initial conditions is

$$u(x,y,t) = \sin(\frac{\pi}{L}x)\sin(\frac{\pi}{L}y)e^{-2\pi^2 t/L^2}.$$

2.7. *Temperature distribution in the lithosphere*

The heat equation describes the temperature distribution in the lithosphere is given by

$$k\nabla^2 T + Q = \rho c_P\frac{\partial T}{\partial t}, \tag{12}$$

where k is the thermal conductivity, Q is the heat production, T is the temperature, ρ is the density and c_P is the specific heat capacity. k, ρ and c_P are constant in this case. To solve this equation using the methods previously discussed in this paper, the equation must be scaled.

2.7.1. *Scaling the heat equation*

By multiplying Eq. (12) we get

$$\nabla^2 T + \frac{Q}{k} = \frac{\rho c_P}{k}\frac{\partial T}{\partial t}.$$

Introducing $D = \rho c_P/k$, and inserting for ∇^2;

$$\frac{\partial^2 T}{\partial x^2} + \frac{\partial^2 T}{\partial y^2} + \frac{Q}{k} = D\frac{\partial T}{\partial t}.$$

Further we assume x and y scale equally, and we introduce dimensionless variables $c = x/\hat{x} = y/\hat{y}$ and insert into the above equation

$$\frac{1}{c^2}\frac{\partial^2 T}{\partial \hat{x}^2} + \frac{1}{c^2}\frac{\partial^2 T}{\partial \hat{y}^2} + \frac{Qc^2}{k} = D\frac{\partial T}{\partial t}.$$

Multiplying by c^2 gives Dc^2 on the right hand side. Since α is a constant we require it to be such that $Dc^2 = 1 \Rightarrow c^2 = k/\rho c_P$. The final scaled equation (where we set $\hat{x} = x$ and $\hat{y} = y$) becomes

$$\frac{\partial^2 T}{\partial x^2} + \frac{\partial^2 T}{\partial y^2} + \frac{Q}{\rho c_P} = \frac{\partial T}{\partial t}. \tag{13}$$

The final model consists of a two dimensional system where the energy only depends on depth, as discussed in section 2.5.4, regarding the boundary conditions. When implementing the radioactive enrichment we add terms that make up the additional heat production to the equation for BE used in Jacobi's method, discussed in section 2.4. The additional heat production depends on the depth as

$$Q = 1.4\mu\text{W/m}^3, \quad 0\text{km} < y \leq 20\text{km}$$
$$Q = 0.35\mu\text{W/m}^3, \quad 20\text{km} < y \leq 40\text{km}$$
$$Q = 0.05\mu\text{W/m}^3, \quad 40\text{km} < y < 120\text{km}.$$

When introducing a radioactive slab located beneath the lithosphere, there is additional heat production over the whole mantle, which stretches over $40 < y < 120$, where y is the depth of the lithosphere. We assume the slab to be 150 km's wide, that means it is sufficiently wide relative to the lithosphere's 120 km width, such that the temperature only depends on depth.

When adding the additional heat term in the 2D diffusion equation solved with Jacobi's method using the BE scheme we consider the additional heat to be a perturbation of previous time step solution. This means we add a constant term to the solution of the previous time step.

It is important to note that the first scaling is in terms of m and s, not Km and GY, so a factor for scaling up the equations is needed. In the program this is implemented as scaling up to $1GY = 60\times 60\times 24\times 365\times 10^9$

and 120000m and factoring this into the α factor. In addition the radioactive perturbations are scaled by factoring 1GY and the time complexity Δt.

3. RESULTS

3.1. *1 Dimensional Diffusion equation*

Results from solving the 1D diffusion equation are shown in Figure 1 and 2.

3.2. *Two dimensional diffusion equation*

Results from solving the 2D diffusion equation are shown in Figure 3.

3.3. *Error in numerical solvers*

Error analysis for the numerical methods are presented in Figure 4, 5, 6, 7 and 8.

3.4. *Diffusion in the lithosphere*

Relevant figures from studying the lithosphere are shown in Figure 10, 11, and 9.

4. DISCUSSION

4.1. *1 Dimensional Diffusion equation*

Figure 1 shows how the numerical solvers give different results with a spatial discretization of $\Delta x = 0.1$. (a) shows solutions at a time t_1, where the heat has not had enough time to spread across the rod. Due to the significant slope of the curve, we can clearly see the differences from employing different numerical solvers. The FE scheme appears to be give less accurate values than the BE and CN schemes, and the CN scheme is slightly more accurate than the BE scheme. From Figure (b) we see that the solutions close to the steady state are less variable, which is most likely due to the temperature change over time being lower.

With a more accurate discretization of the rod (Figure 2), the solutions from the implicit methods BE and CN are indistinguishable from the analytical solution. The FE method is still noticeably less accurate than the other methods. From this we can say that the implicit methods are preferable in terms of numerical accuracy.

This is investigated further by plotting absolute error along the 1D rod for two different times and two different resolutions of Δx. This is done in Figure 4 and Figure 5 in logarithmic scale. Reviewing the graphs it becomes clear that for lower resolutions $\Delta x = 0.1$ the CN method slightly outperforms BE along most of the rod. This however is contrasted when analyzing the same rod with a higher resolution where BE seems slightly better.

4.2. *2 Dimensional Diffusion equation*

Figure 3 shows the temperature for every grid point using a contour plot. As expected, the initial state shown in the (a) has more heat close to the center, as this is where the heat propagates from. The heat then dissipates through the boundaries until a steady state is reached, as shown in (b). At this point, the temperature no longer changes over time. Since the temperature at the boundaries are set to 0 everywhere the edges function as drains for the heat causing all heat to escape the system. When the steady state is reached the temperature is uniformly zero.

4.3. *Forward Euler vs. Backward Euler schemes in 2D*

The difference in computed temperatures between analytic and FE (a) and analytic and BE (b) methods are displayed in Figure 6. The absolute difference between the analytic and FE is at most roughly 0.20 as shown by the color bar. Towards the boundaries the difference decreases to zero. The difference with the BE solution is close to 0 everywhere, but we see some difference, especially close to the center. Because of the larger error relative to the analytic solution we discarded the FE solver for later results and focused on BE. The stability of the BE solver for different values of $\alpha = \frac{\Delta t}{\Delta x^2}$ can be seen in Figure 7 and 8. For a 100×100 grid, we see the absolute error increasing as α increases, as this corresponds to lower resolution in time. However, the error is never more than 0.01 which suggests that the algorithm is stable.

For a 10×10 grid, we see that the error does not always increase as α increases. While we expect a lower α to give more accurate results, the spatial resolution might be too low for this to be true. Figure (a) with $\alpha = 0.25$ should theoretically give the best result, but this is not the case. Figures (b) and (c) give more accurate results while figures (d), (e) and (f) give errors of around 0.6, which is very high.

4.4. *Diffusion in the lithosphere*

In Figure 10 the initial state displayed is the steady state with a linearly increasing gradient. Assuming that the area simulated are contained within a reservoir in steady state, we simulate the system with its boundary conditions preserved. The gradient does not change throughout the simulation and we can assume this is one way of reasonably modeling the steady state without the radioactive heat generating perturbations.

Analyzing the case of radioactive heat generation as seen in Figure 11 (a) the heat in the system increases considerably. We still simulate under the assumption that the boundary conditions are conserved, this may lead to inaccuracies in the heat distribution of the system. One possible solution to that problem would be to

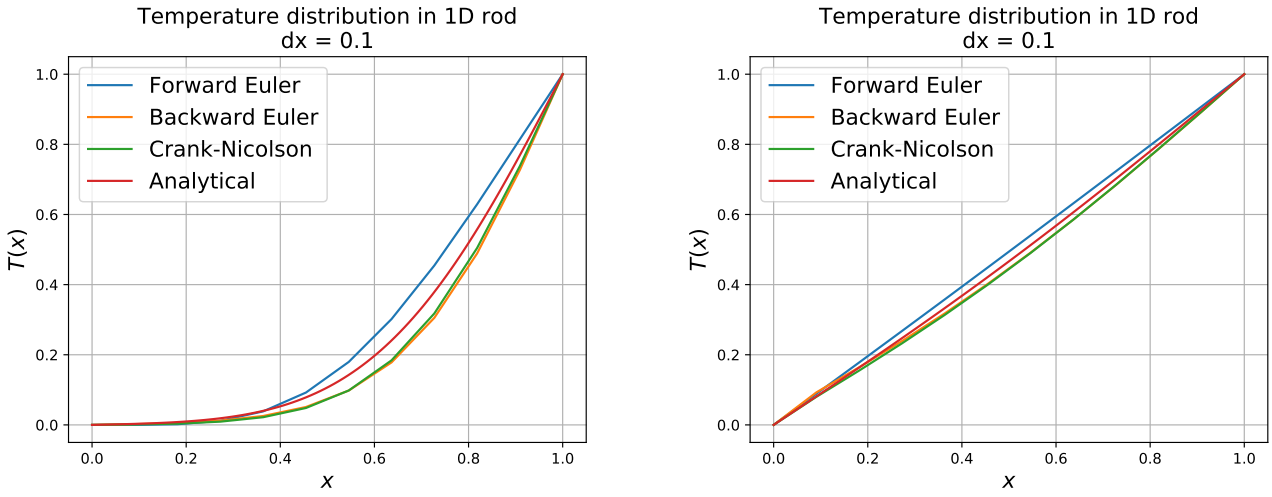

(a) (b)

Figure 1. Numerical solution of the 1D diffusion equation using different numerical solvers compared to the analytical solution. Boundary conditions are $T(0,t) = 0$ and $T(L,t) = 1$. The solutions to the left are computed at a time t_1, where $t_1 < t_2$. The solutions to the right are computed at a time t_2, where a steady state has almost been reached. The time step is defined through the constraint on the explicit FE scheme (Eq. (5)).

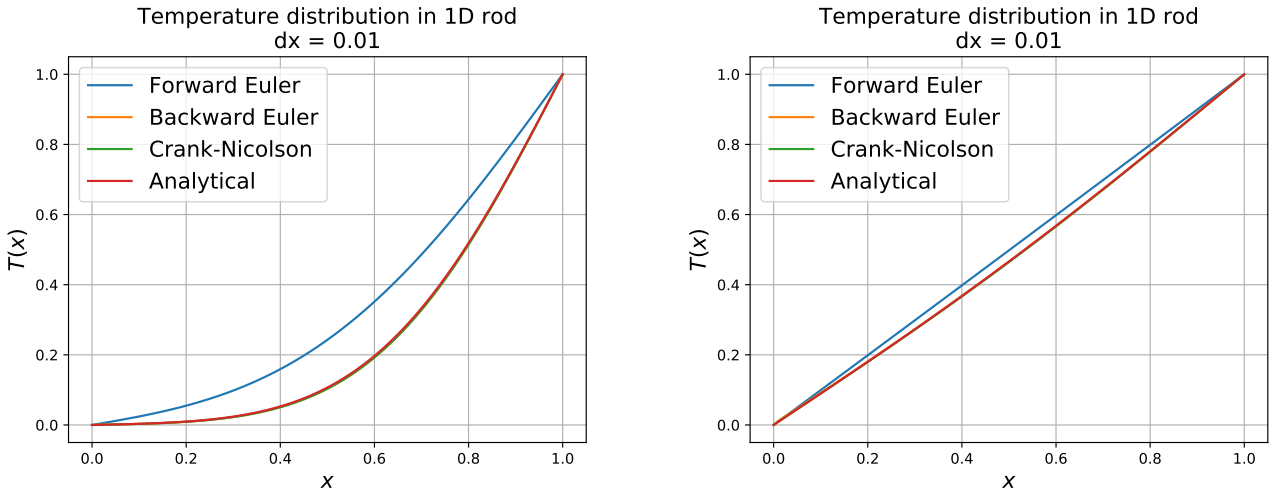

(a) (b)

Figure 2. Numerical solution of the 1D diffusion equation using different numerical solvers compared to the analytical solution. Boundary conditions are $T(0,t) = 0$ and $T(L,t) = 1$. The solutions to the left are computed at a time t_1, where $t_1 < t_2$. The solutions to the right are computed at a time t_2, where a steady state has almost been reached. The time step is defined through the constraint on the explicit FE scheme (Eq. (5)). An animation can be found on github: https://git.io/fpbRR.

implement periodic boundary conditions, however the results look otherwise reasonable in the center of the system. The gradient starts in the same initial state as the linear case, but develops quickly over time before reaching steady state after about 0.16 GYr.

The last case it that of the slab enriched in U, Th and K, this situation depicted in its steady state in Figure 11 (b). We assume that since the reduction of radioactive material due to decay is low in 1 GYr, the simulation is run without actually considering the decay at all. Boundary conditions are still a source of error, however again along the center of the system the results are still seemingly reasonable. The temperature increases even faster than earlier and when it reaches steady state, about 0.18 GYr, the temperature exceeds $1300°C$ in some places.

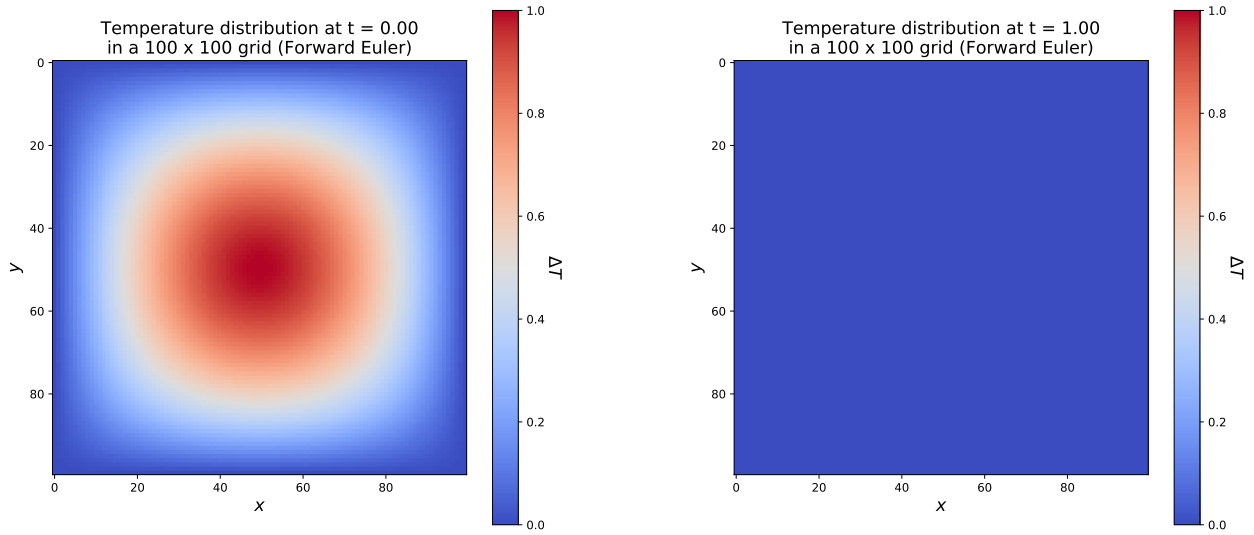

(a) (b)

Figure 3. Numerical solution of the 2D diffusion equation using an explicit FE scheme, with boundary conditions $T(x,0,t) = T(x,L,t) = 0$ and $T(y,0,t) = T(y,L,t) = 0$. The time step is defined using Eq. (5). The figure on the left (a) shows the initial state, with initial condition is set to $u(x,y,0) = sin(\pi x)sin(\pi y)$. There are larger amounts of heat closer to the center of the system. (b) shows the temperature distribution after a steady state has been reached. An animation can be found on github: https://git.io/fpbuv.

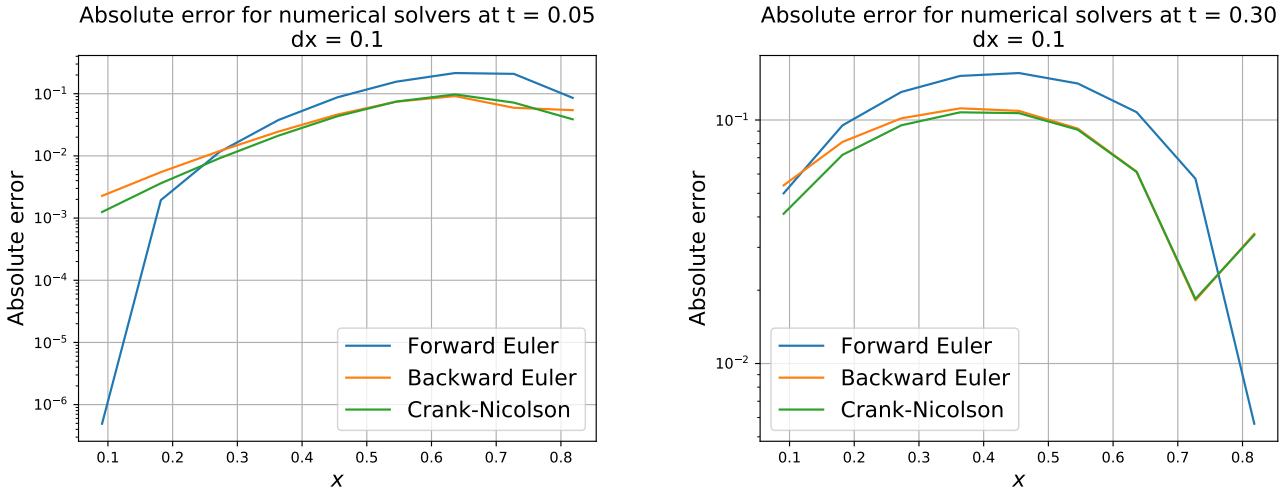

(a) (b)

Figure 4. Absolute error from using different numerical schemes with $\Delta x = 0.1$. The error in (a) is computed at a time t_1, where $t_1 < t_2$. Figure (b) was computed at a time t_2, where a steady state has almost been reached.

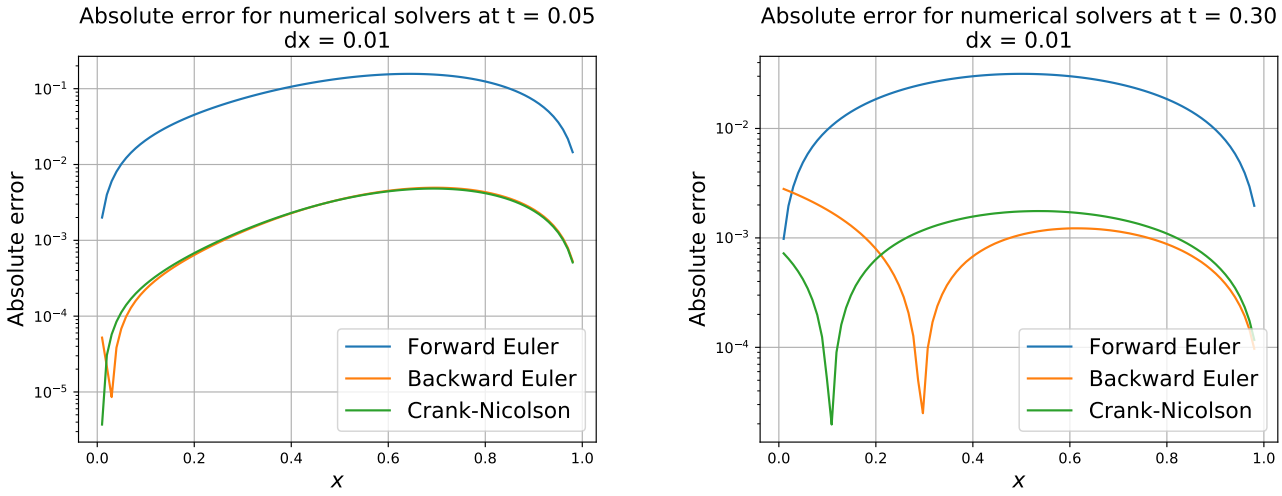

(a) (b)

Figure 5. Absolute error from using different numerical schemes with $\Delta x = 0.01$. The error in figure (a) is computed at a time t_1, where $t_1 < t_2$. Figure (b) was computed at a time t_2, where a steady state has almost been reached.

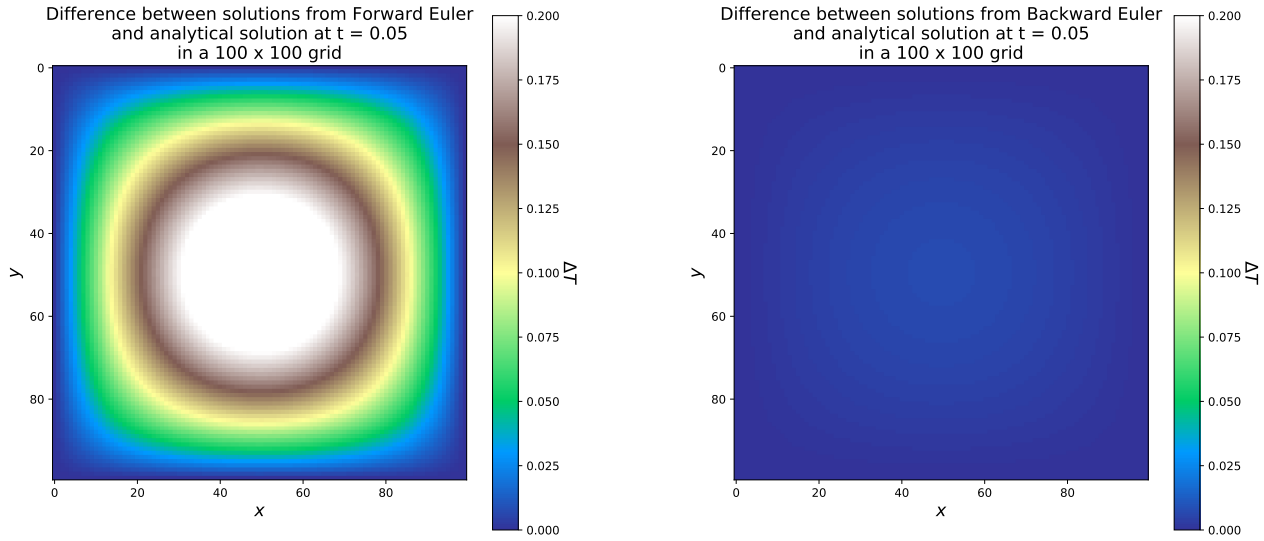

(a) (b)

Figure 6. Heat maps of numerical error from FE and BE schemes in two dimensions. The physical conditions are the same as in Figure 3. An animation of (a) and (b) can be found at github on https://git.io/fpb0x and https://git.io/fpb0Q respectively.

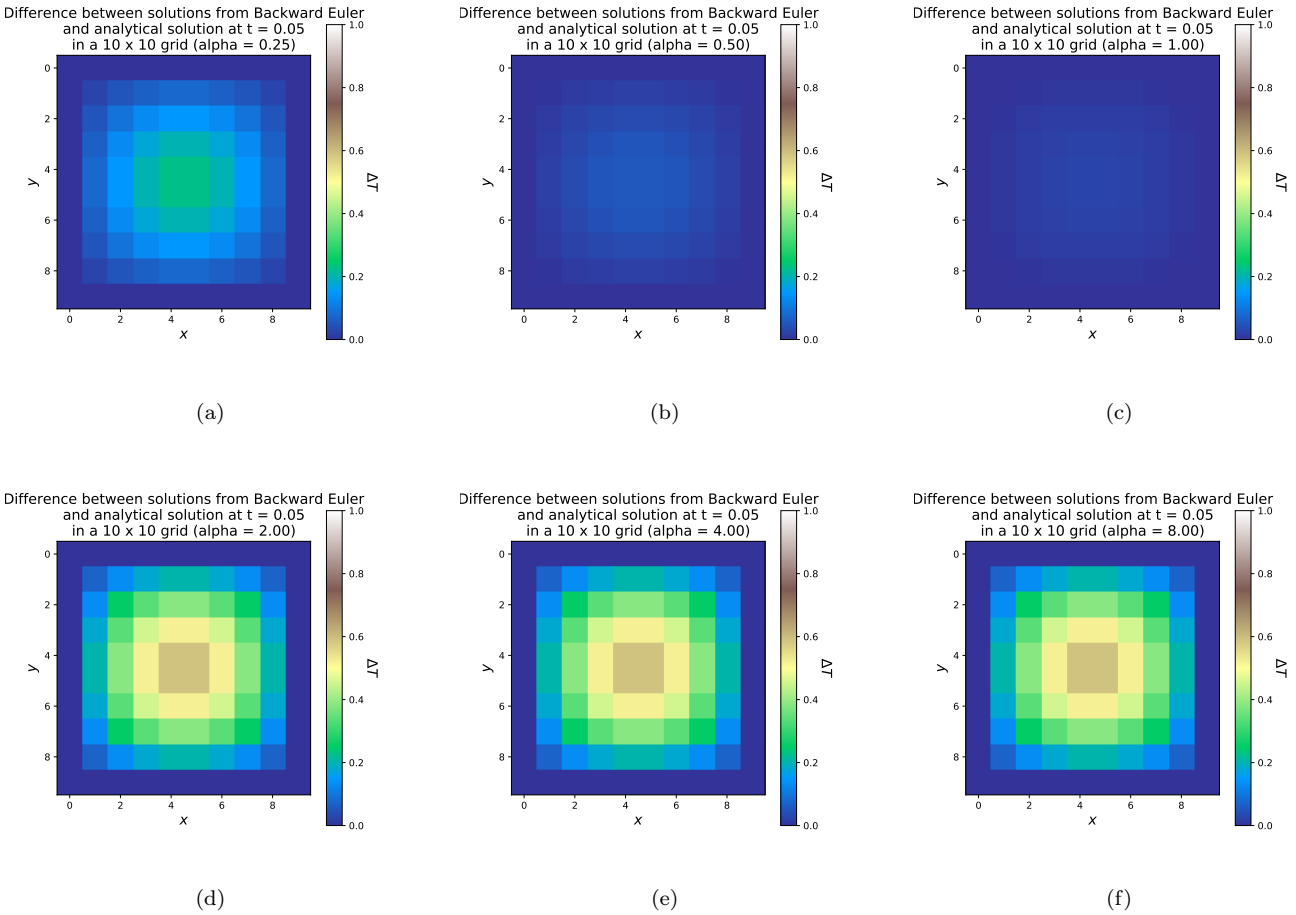

Figure 7. Absolute error of the BE scheme at a time $t = 0.05$ using different values of α, with $\Delta x = \Delta y = 0.1$.

Reviewing Figure 9 we see a comparison between the temperature distributions in a slice of the center of the lithosphere after 1 GYr. As expected in the case of the enriched mantle, the temperature further down $(40 < y < 120)$ exceeds $1300°C$, while it converges with the non-enriched solution towards the lowest $8°C$ in the upper crust. The higher heat production in the upper crust results in the non-enriched radioactive system to converge towards the lowest temperature at a slower rate than otherwise, this is seen as the turning points in the graph.

5. CONCLUSIONS

After studying the use of explicit and implicit methods to solve partial differential equations in one and two dimensions, we have found that.

The one dimensional diffusion equation is best solved with the implicit BE and the implicit CN scheme rather than the FE scheme. Using the explicit FE scheme, significant numerical errors arise even with the constraint $\alpha = \Delta t/\Delta x^2 \leq 1/2$ set appropriately. The BE and CN scheme are about the same in terms of precision, with some minor differences as shown in Figure 7 and 8.

Jacobi's method works well as implicit solver in the 2D case, given that the initial conditions and boundary conditions are chosen reasonably. Our results shows that the error in the method scales with Δx which is about $1/100$. However it is important to note that the method should be parallelized if one wishes to work with larger matrices. Parallelizing should be fairly straight forward as the rows in the matrices can be calculated independently.

When extending what was done with Jacobi's method to a model of a geological system, we chose to preserve boundary conditions. While the results were not entirely realistic (seen in 11) we found that our solution achieved reasonable results in a cross-section in the center of the system as seen in figure 9.

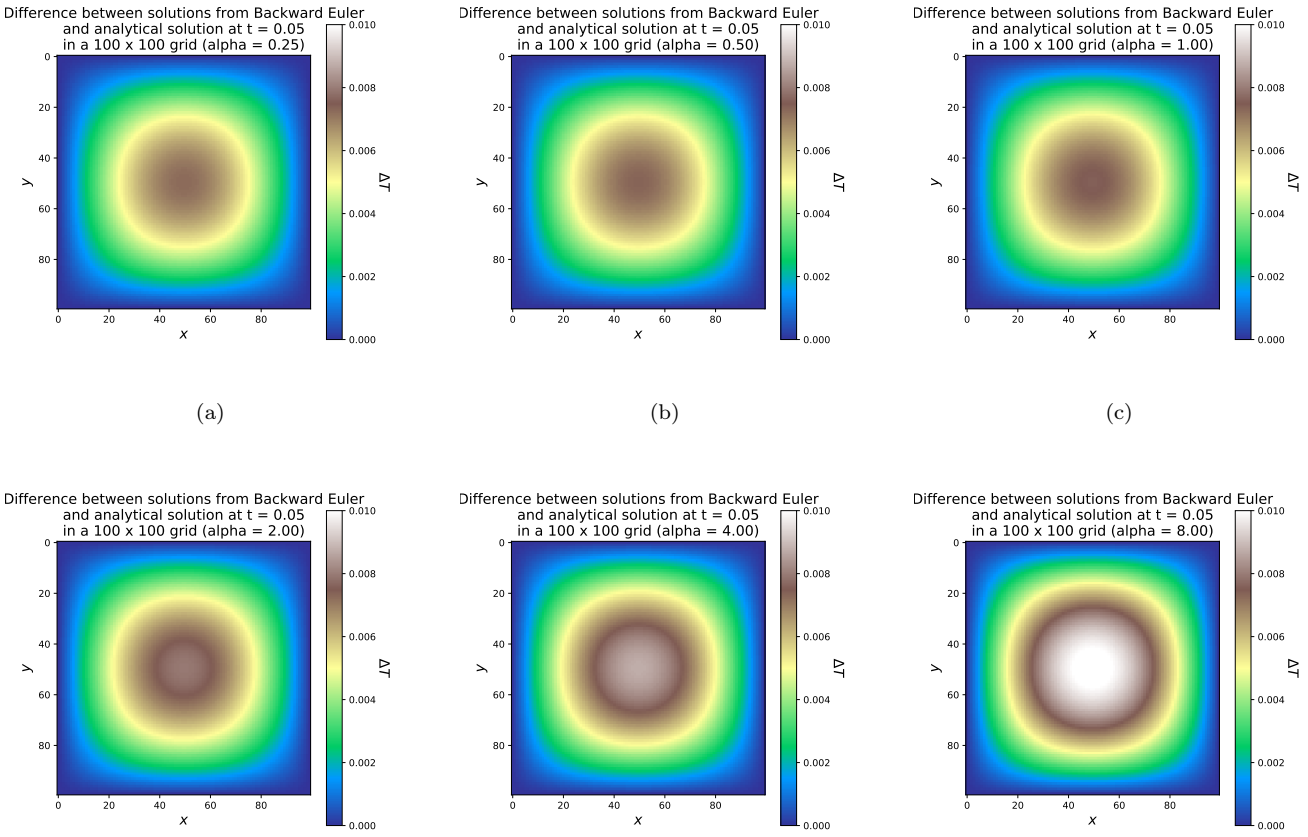

(a) (b) (c)

(d) (e) (f)

Figure 8. Absolute error of the BE scheme at a time $t = 0.05$ using different values of α, with $\Delta x = \Delta y = 0.01$.

REFERENCES

Hjorth-Jensen, Morten, 2018, *Project 5* http://compphysics.github.io/ComputationalPhysics/doc/Projects/2018/Project5/DiffusionEquation/pdf/DiffusionEquation.pdf

Hjorth-Jensen, Morten, 2015, *Lectures 2015* https://github.com/CompPhysics/ComputationalPhysics/blob/master/doc/Lectures/lectures2015.pdf

Foyn, Stig-Nicolai, Dreierstad, Christer 2018, *Project 1* https://github.com/chdre/FYS3150/blob/master/Project1/report/FYS3150-Project1-stignicf-chrisdre.pdf

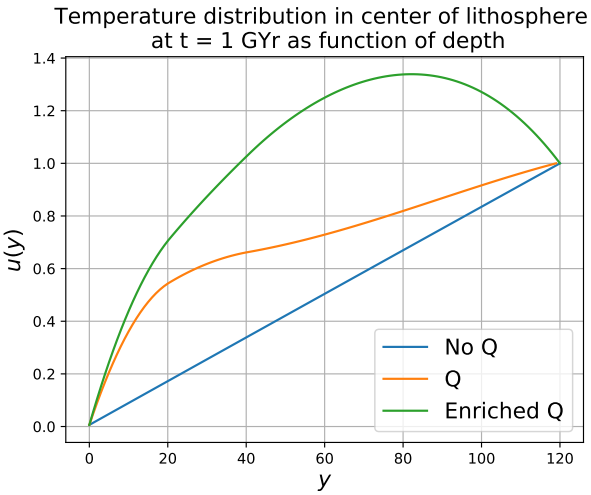

Figure 9. Steady state along the cross section (for L/2 in x-direction) of the lithosphere for the three cases 1) no additional thermal perturbations 2) radioactive thermal perturbation 3) enriched radioactive thermal perturbation in the mantle.

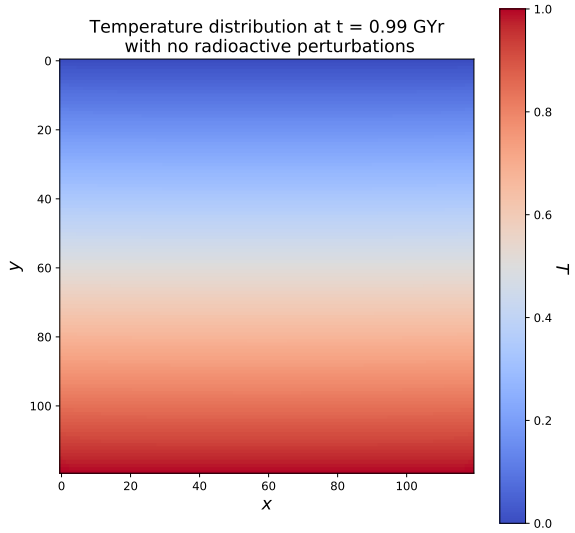

Figure 10. Temperature distribution of the steady state system with boundaries $T(x,0,t) = 8°C/1300°C$ and $T(x,L,t) = 1$. Initial condition is such that the temperature increases from top to bottom with a change $\Delta T = i(1-8/1300)/120$, $1 \leq i \leq 120$. $\Delta x = 1/120$, $dt = 1/(\Delta x)^2$. An animation can be found on github: https://git.io/fpbEs.

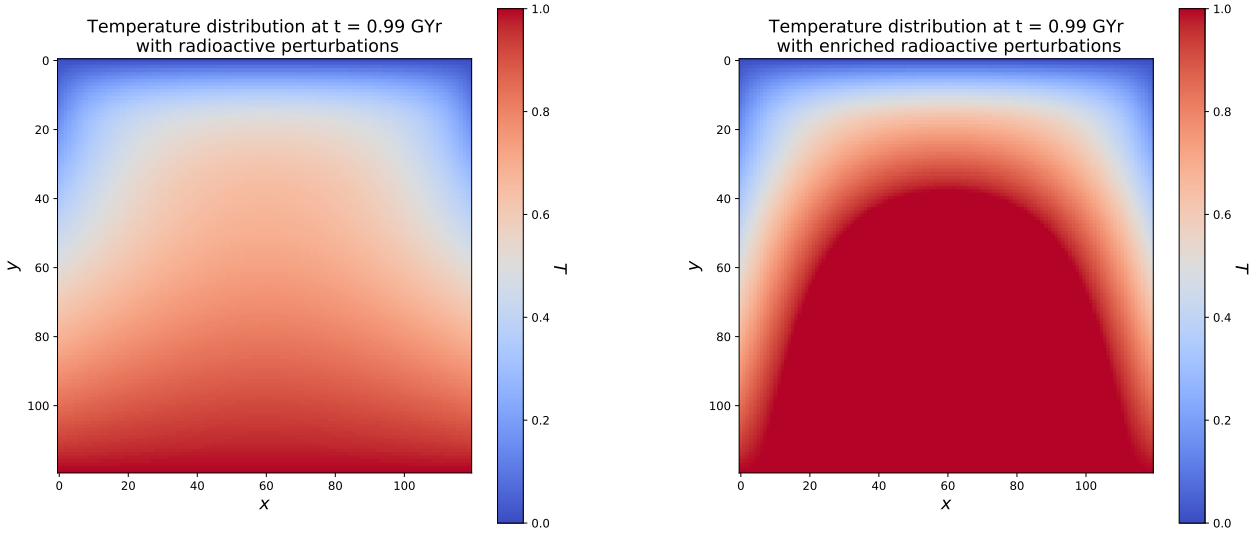

(a) (b)

Figure 11. Temperature distribution of the steady state system with radioactive thermal perturbations. The system starts in the same initial conditions and the boundaries along along both axes are conserved. The radioactive perturbations are scaled up from what is seen in 2.7.1. For figure (b) the radioactive perturbations along the last interval has an additional enrichment term of $Q_{enrich} = 0.5\mu W/m^3$. Animations for no slab and slab can be found on github: https://git.io/fpbE0 and https://git.io/fpbEa respectively.